Volume 1 | Issue 1 | 2019 April | ISSN 2661-331X (Online)

Hydro Science & Marine Engineering

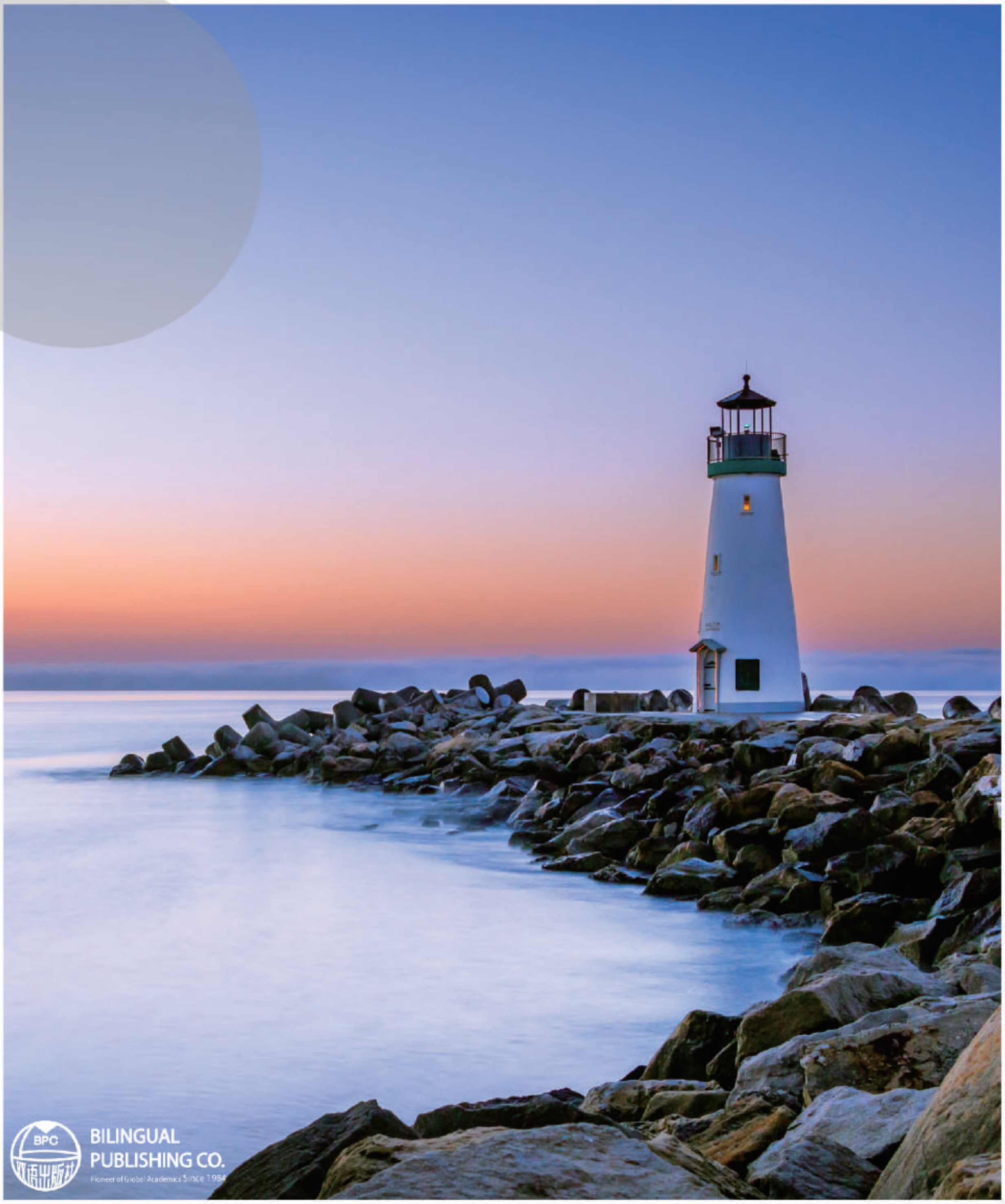

1 • 2019

Volume 1 Issue 1 · April 2019 · ISSN 2661-331X (Online)

Hydro Science & Marine Engineering

Editor-in-Chief

Dr. Ming Zhao

BILINGUAL PUBLISHING CO.
Pioneer of Global Academics Since 1984

Volume 1 | Issue 1 | April 2019 | Page 1-21
Hydro Science & Marine Engineering

Contents

Editorial

Article

Hydro Science & Marine Engineering
https://ojs.bilpublishing.com/index.php/hsme

EDITORIAL

Forward for Inaugural Issue of Hydro Science & Marine Engineering

Ming Zhao*

Western Sydney University, Australia

ARTICLE INFO

Article history
Received: 28 October 2019
Accepted: 29 October 2019
Published Online: 31 October 2019

It is with great pleasure that we present this inaugural issue of Hydro Science & Marine Engineering (HSME), a peer-reviewed journal for academics to freely disseminate research findings in areas including but not limited to; Marine Biotechnology, Irrigation and Drainage, Ocean Engineering, Coastal and Offshore Engineering, Hydraulics, Surface and Groundwater Hydrology, Sediment Transport, Climate Change, Water Quality and Pollution control, Coastal Protection and Lake/Shore Environment. High standard research and developments in the above areas are crucial for sustainable development and environmental protection. The mission of HSME is to provide researchers with an ideal forum to publicize academic research and exchange information on all the above topics.

We welcome research articles with academic contributions through different formats of research including theoretical analysis, numerical simulations, experimental studies, fields tests, applied research, case studies, reviews, and so on. The journal is published under the Open Access model, which allows for the greater dissemination of research results by granting free access to the public. The Open Access increases the citation and impact factor of the published article. Under the Creative Commons Attribution License (CC BY), the author retains the copyright of the content and the public is allowed to adapt and share the author's content, as long as the author is properly credited.

The journal's editorial team consists of leading experts across the world. The editorial board is dedicated to ensuring that the peer-reviewing process of the articles conforms to the international standard expected by the scientific research community. To reflect our interest in quickly publishing top quality papers with significant impact, we give priority to the papers that are highly valued by the reviewers. HSME is a semi-annual publication. In addition, we will periodically publish special issues that are focused on research on interesting topics within specific disciplines. The special issues provide an ideal platform for dissipating research on emerging areas, important science and engineering issues, or cross-disciplinary applications.

We are committed to, through rapid and high-standard peer-review processes, to finding a home for papers that report new theories, new methods, new discoveries, new applications and reviews. I sincerely appreciate the great contribution from the authors and reviewers to this inaugural issue. With the enthusiasm and supports from authors, reviewers, readers and editors, I strongly believe HSME will achieve great success. Finally, I would like to invite authors in all the research communities to submit their research papers to this exciting journal.

**Corresponding Author:*
Ming Zhao,
Western Sydney University, Australia;
Eamil: m.zhao@westernsydney.edu.au

Hydro Science & Marine Engineering
https://ojs.bilpublishing.com/index.php/hsme

ARTICLE

Influence of Long-term Climate on Fatigue Life of Bridge Pier Concrete and a Reinforcement Method

Nam-Hyok Ri[1,2,3*] Kum-Hyok So[2] Yong-Sop Ri[2] Zhiyao Ma[1] Yong-Ae Kim[2] Hui-Gwang Yun[4]

1. School of Architecture, Tianjin University, Tianjin, 300072, China
2. Faculty of Mechanics Engineering, Kim Il Sung University, Pyongyang, DPR of Korea
3. School of Civil Engineering, Tianjin University, Tianjin, 300072, China
4. Department of Resources Exploration Engineering, Kim Chaek University of technology, Pyongyang, DPR of Korea

ARTICLE INFO

Article history
Received: 9 July 2019
Accepted: 30 September 2019
Published Online: 31 October 2019

Keywords:
Hydraulic concrete
Bridge pier
Concrete depression failure
Scour phenomenon; Low-cycle fatigue life
Long-term climate
Thermal-structural analysis
Fluid-structural analysis
ANSYS

ABSTRACT

This paper quantitatively evaluated the fatigue life of concrete around the air-water boundary layer of bridge piers located in inland rivers, considering the long-term climate. The paper suggests a method to predict the low-cycle fatigue life by demonstrating a thermal-fluid-structural analysis of bridge pier concrete according to long-term climate such as temperature, velocity and pressure of air and water in the process of freezing and thawing in winter. In addition, it proposes a reinforcing method to increase the life of damaged piers and proves the feasibility of the proposed method with numerical comparison experiment.

1. Introduction

The depression failure of concrete surface around the air-water boundary of bridge pier is a common damage phenomenon appears in old bridges. These concrete surface failures are caused by various factors such as construction defect, cycled fatigue loads [1,2], corrosion of reinforcement steel bar [2-5], aggressive climate change [6-8] and so on. If the factor of construction defect is excluded, the failure of bridge piers located in marine zone is mainly influenced by the accelerated corrosion of reinforcement steel bars due to the salt composition [3-5] and the failure of bridge piers located in inland zone is mainly influenced by freezing and

**Corresponding Author:*
Nam-Hyok Ri,
School of Architecture, Tianjin University, Tianjin, 300072, China; Faculty of Mechanics Engineering, Kim Il Sung University, Pyongyang, DPR of Korea; School of Civil Engineering, Tianjin University, Tianjin, 300072, China;
Email: mech05@ryongnamsan.edu.kp

DOI: https://doi.org/10.30564/hsme.v1i1.1009

thawing due to the temperature difference of the morning and evening in cold winter [7]. Many experimental and theoretical researches were achieved on the fatigue strength of hydraulic concretes under the ordinary or low temperature conditions [7,9]. Some experiments proved that the influence of long-term freezing and thawing due to the temperature difference of morning and evening in cold winter on the fatigue life of old bridge concrete cannot be ignored. In other words, even though the thermal stresses generated during the freezing and thawing process are not larger than the limits of static concrete strength, but it is clear that they are in the range of stress to cause low-cyclic fatigue failure of old concrete [7,9]. There are few researches on the qualitative analysis about the influence of freezing and thawing on the fatigue life of concrete pier, however, those on quantitative analysis has never been performed [6,7]. Based on these previous works, this paper analyzes the stress of old bridge concrete using the thermal-fluid-structural analysis, estimates the fatigue life quantitatively, and proposes a proper reinforcing method to increase the life of pier.

2. Materials and Methods

The case study is “Ch” Railway Bridge constructed in 1975. The diameter of piers is 4 m, the height of the tallest pier is 22.3 m. The piers No. 12 and 13 of the bridge were reinforced with non-reinforcement concrete, where no reinforcement steel bar was used, because of construction defects in 1976. After that, there occurred twice of concrete depression failures and twice of reinforced construction were performed with non-reinforcement concrete in 1988 and 2001. However, in 2014, the old reinforced layer of concrete has been damaged into the original depth again. (Figures 1 and 2 [10])

Based on the atmospheric and hydro materials in recent 10 years, the air temperature curve, wind velocity curve and water temperature curve are interpolated into various functions by MATALAB [11]. (Figures 3-5) All points in graphs are average values per day.

Table 1 shows the thermal properties and structural properties of pier concrete and reinforcement steel.

The analysis time is one year (from 1st of January to 31st of December) and the analysis objects are dynamical temperature field, fluid feild and stress field. In order to investigate the change of thermal stress due to the temperature difference between morning and evening, the time step is set to half of a day, which is the time interval between 2:00 am, when the temperature decreases to the lowest and 2:00 pm, when the temperature increases to the highest.

The river depth and flow velocity are assumed to be constant in a year, excluding the rainy season.

The average velocity of water flow is 2 m/s on the outer layer of the river flow (on the two-phase boundary of water and air (Figure 6)), and is 0 on the bottom of the river flow (on the boundary of water and ground). The liquid flow is assumed to be the Newton viscous flow, in other words, the velocity distribution is assumed to be linear from the ground to the outer layer.

In order to simulate the river flow, the Open Channel Flow is applied by VOF (Volume of Fluid) of ANSYS Fluent and the RNG k-ε turbulent flow model is used for modeling the fluid flow in the Pressure Based Solver tool.

The velocity field and the pressure field around the pier are analyzed by ANSYS. (Figures 7 and 8).

Based on the wind velocity (Figure 4) and the water flow velocity (Figure 7), the convection coefficients are calculated by the followed equations:

$$k_a = k_{an} + k_{af} v_a \quad (1)$$

$$k_w = k_{wn} + k_{wf} v_w \quad (2)$$

where k_a and k_w are convection coefficients, k_{an} and k_{wn} are natural convection coefficients, k_{af} and k_{wf} are forced convection coefficients and v_a and v_w are flow speeds of air (wind) and water (river).

The results of temperature field of thermal analysis and pressure field of fluid analysis at every step of time increment are changed into the thermal-structural boundary conditions of the structural analysis and the Drucker-Prager plastic model is used for analyzing elasto-plastic behavior of concrete in the transient structural analysis solver.

On the basis of above materials and methods, the sequential transient thermal-fluid-structural analysis is performed by ANSYS [12] and fatigue life is predicted by MATLAB.

3. Ethics Statement

The study was approved by the National Program on Key Science Research of the DPR of Korea. The work described has not been submitted elsewhere for publication, in whole or in part, and all the authors listed have approved the manuscript that is enclosed. I testify to the accuracy on behalf of all the authors.

4. Results

4.1 Fatigue Life Prediction of Sound Pier Concrete

Analysis results of temperature field and stress field of sound pier

Figure 9 is the finite element model of the sound bridge pier and Figure 10 is the temperature field and stress field at the moment of the lowest temperature in winter (at 2:00 am on January 15).

Figure 11 is the change curve of the 1st principal stress along the radial direction inside the bridge pier at the height of the air-water boundary layer and Figure 12 is the change curve of the 1st principal stress along the vertical direction on the outside surface of pier.

Figure 11 shows that the stress increases rapidly from the center to the outside surface of the pier and Figure 12 shows that the stress on the concrete surface of the air-water boundary layer changes sharply from compress to tensile. From this, it can be seen that the 1st principal stress becomes maximum on the concrete surface of the water-air boundary layer.

Figure 13 is the change curve of stress on the concrete surface on the air-water boundary layer in a year, which shows the season when the stress changes most aggressively is winter, that is, from November 15 to February 15, respectively.

Figure 14 shows the change of the 1st principal stress from November 15 to February 15 in detail.

4.2 Fatigue Life Prediction of Sound Pier Concrete

In general, the fatigue strength of the concrete increases as the temperature decreases. To predict the fatigue life, the paper uses Eq. (3), a fatigue life calculation formula of hydraulic concrete considering the effect of temperature [9]:

$$\lg N = C(t)\frac{1-S_{\max}}{1-S_{\min}/S_{\max}} \tag{3}$$

, where N is the number of load cycles and C(t) is the coefficient related to the environment such as temperature, which is generally in the range of 10 to 20. It takes 14.6 at 20 ° C and 20 at -24 ° C in case of C45 concrete. $S_{\max}$ and $S_{\min}$ are the ratios of the maximum and minimum stresses to the concrete strength in static state. Considering that C(t) is a monotonic function according to temperature and that the range of the temperature change is not large, the function of C(t) can be interpolated into a linear function of $C(t) = at + b$, where $a \approx -0.0614$, $b \approx 8.5274$. So, Eq. (3) can be rewritten as follow.

$$\lg N = (-0.0614t + 8.5274)\frac{1-S_{\max}}{1-S_{\min}/S_{\max}} \tag{4}$$

By using Eq. (4) and the graph of stress change according to the time (Figure 11), the change curve of fatigue life according to the stress amplitude per day in a year can be obtained. (Figure 15)

Figure 16 shows that the limit number of load cycles in the sound bridge pier is at least $10^{3.7}$ times (more than 70 years) under the condition that the depth and flow path of river do not change.

4.3 Fatigue Life Prediction of Reinforced Pier Concrete

The comparison between the previous reinforcing method with non-reinforcement concrete and this paper's reinforcing method with reinforcement concrete is performed. The previous reinforcing method is to reinforce the pier with non-reinforcement concrete of 80 cm thickness on the outer surface of the original damaged pier. The paper's reinforcing method is to reinforce the pier with reinforcement concrete of 30 cm thickness on the outer surface of the original damaged pier. The diameter of reinforcement steel bars is 12 mm and they placed under the depth of 5 cm from the outer surface of reinforcing layer. There are arranged 48 reinforcement steel bars in the hoop direction and 10 reinforcement steel bars per 3 m in the axial direction of the pier.

On the two reinforcing methods, the values of 1st principal stress and their changes on the outside surface of reinforced layer are similar. (Figure 16) (They are 1.5 times larger than the stress of sound pier.)

However, the fatigue lives do not equal (Figure 17). Figure 17 shows that the limit number of load cycles in the bridge pier reinforced with non-reinforcement concrete is 10^3 times (more than 15 years) and one in the bridge pier reinforced with reinforcement concrete is $10^{3.4}$ times (more than 50 years) under the condition that the depth and flow path of river do not change.

5. Discussion

The above results show that the reinforcing method with reinforcement concrete can increase the fatigue life. It is about 3.5 times more than on the reinforcing method with non-reinforcement concrete. (Figure 17)

Moreover, the reinforcing method with reinforcement

DOI: https://doi.org/10.30564/hsme.v1i1.1009

concrete can reduce the effect of scouring phenomenon at the bottom of the pier, which greatly influence on the stability and buckling of the pier. The reinforcing method with reinforcement concrete can increase the safety factor against the scour phenomenon because the thickness of the reinforcement concrete layer is much thinner than one of the non-reinforcement concrete layer.

6. Conclusion

This paper quantitatively predicted the damage and fatigue life of concrete around the air-water boundary surface of bridge piers located in inland rivers, considering the thermal stress fatigue effect due to the long-term climate.

(1) The most aggressive position to the thermal fatigue of bridge pier concrete due to freezing and thawing in cold winter is the zone around the air-water boundary layer of the pier.

(2) The occurrence of fatigue cracking should be predicted in about 70 years under the condition that the depth and the flow path of river do not change.

(3) On the reinforcing method with non-reinforcement concrete, the fatigue cracking should be predicted in about 15 years under the condition that the depth and the flow path of river do not change.

(4) On the reinforcing method with reinforcement concrete, the fatigue life increases to 3.5 times (about 50 years), the safety factor against the scour phenomenon increases to 1.2 times, and the amount of required concrete for reinforcing decreases to 33 %, compared to the non-reinforcement concrete within the same strength.

Author Contributions

N. R. conceived the idea and performed theoretical calculations and numerical simulations. Y. R. supervised the project. Y. K. and H. Y. investigated the practical materials. K. S. and Z. M. contributed to preparation of the manuscript.

Acknowledgement

The research was supported by the National Program on Key Science Research of the DPR of Korea. (Grant No. 0305014-01) I would like to thank all the researchers, designers and engineers in this project for their great help. I would like to express my wholehearted gratitude to my conductor Prof. Chen Zhihua and Prof. Ma Zhiyao of the Tianjin University, China for their selfless advices to my research. I also thank to Dr. Sim Song-Jun, the Chief of English Department of Pyongyang University of Foreign Studies for his great help in my paper in English.

Appendixes

Table

Table1. Thermal and structural properties of concrete and steel

Properties Pier concrete		Material	
		Reinforcement steel	
Thermal properties	Specific heat (J/kg/℃)	1004.8	455
	Heat conductivity (W/m/℃)	2.675	80
	Expansion coefficient (10^{-5}/℃)	1	1.1
Structural properties	Density (kg/m^3)	2470	7850
	Young's ratio (GPa)	20	200
	Poisson's ratio	0.167	0.3

Figures

Figure 1. Damaged bridge pier

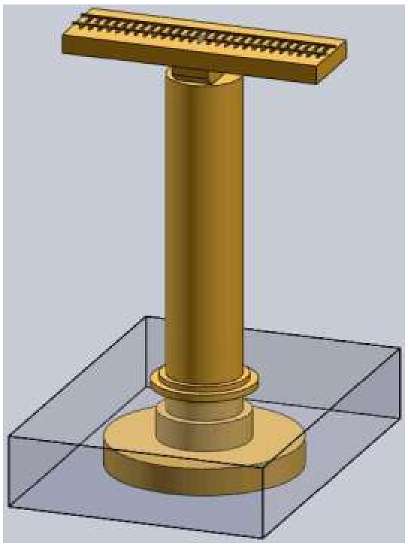

Figure 2. Geometric model of damaged pier

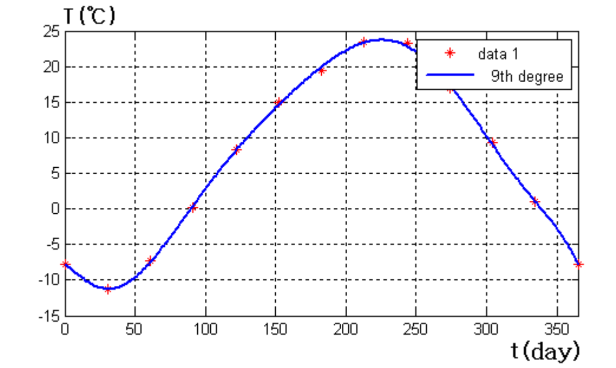

Figure 3. Daily average air temperature changes in a year

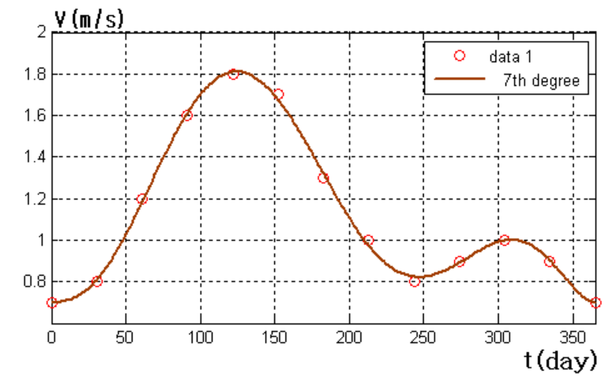

Figure 4. Daily average wind speed change in a year

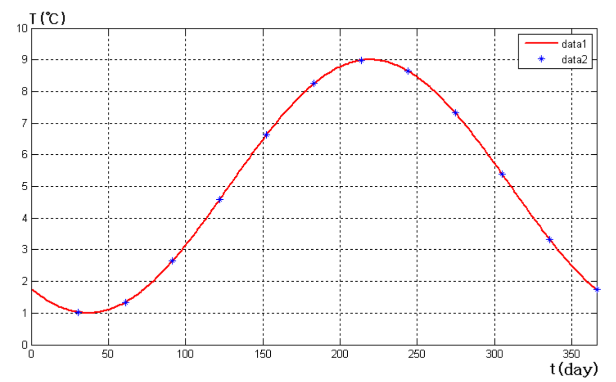

Figure 5. Daily average water temperature changes in a year

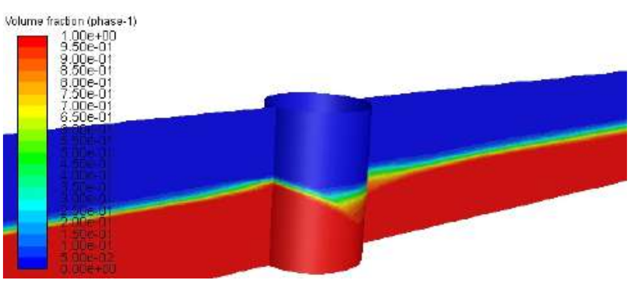

Figure 6. Volume fraction distribution on the air-water two-phase flow

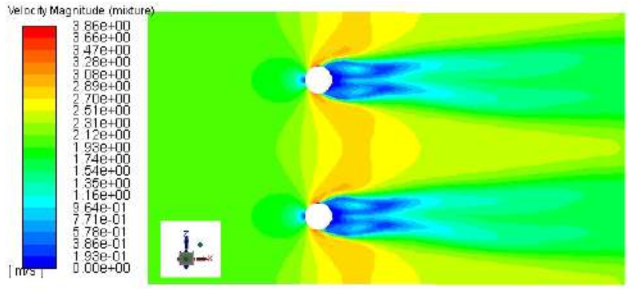

Figure 7. Water flow velocity field around the pier (on the depth of 1 m)

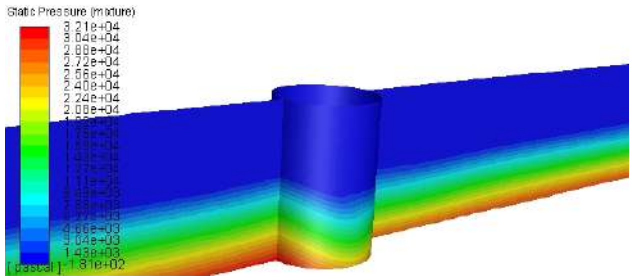

Figure 8. Water pressure field around the pier

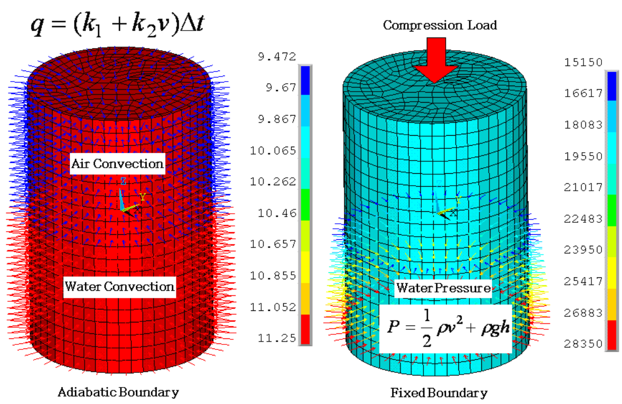

Figure 9. Finite element model

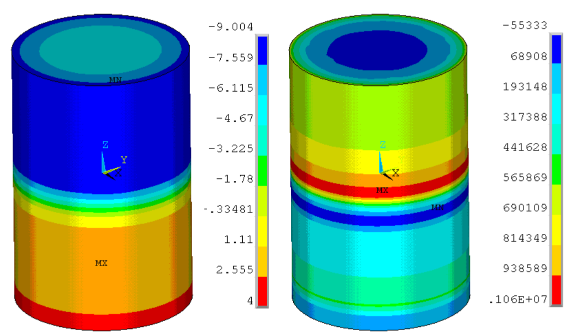

Figure 10. Temperature field and stress field of the pier

DOI: https://doi.org/10.30564/hsme.v1i1.1009

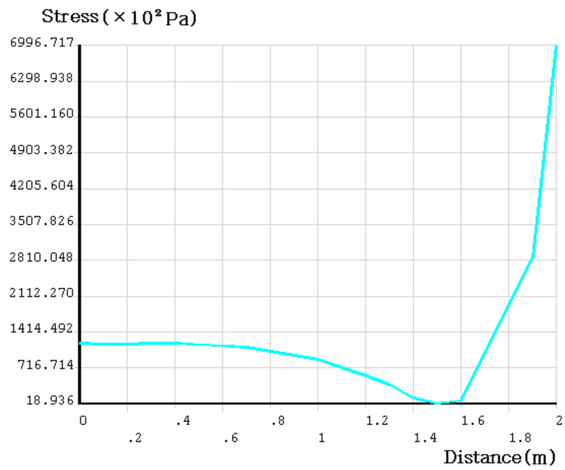

Figure 11. 1st principal stress change in radial direction

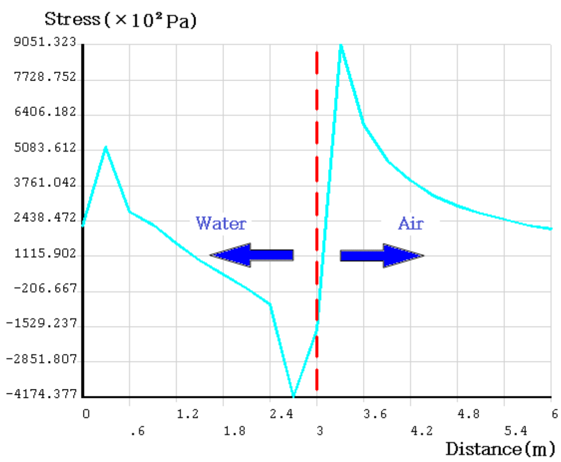

Figure 12. 1st principal stress change along the height

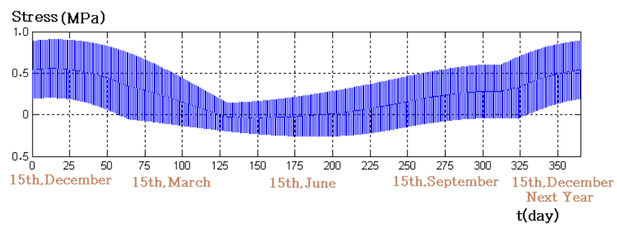

Figure 13. 1st principal stress change curve on the air-water boundary surface in a year

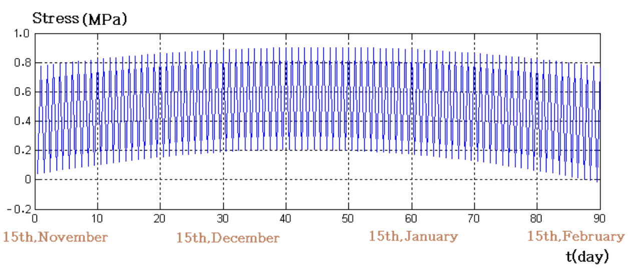

Figure 14. 1st principal stress change curve on the air-water boundary surface in winter

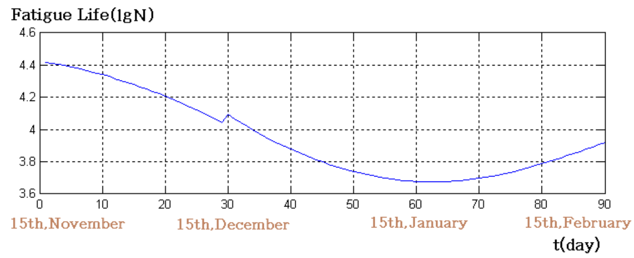

Figure 15. Fatigue life change of pier concrete according to day

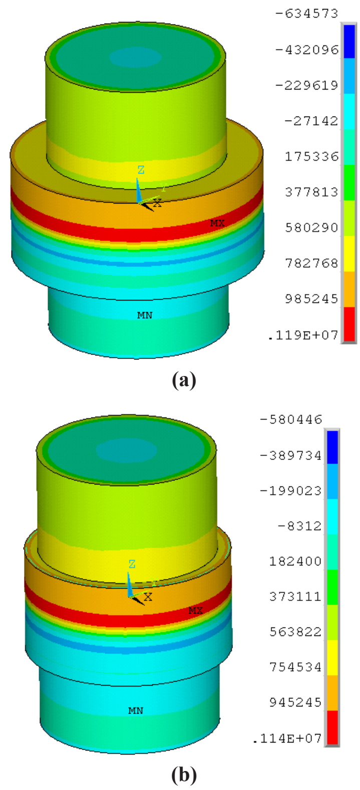

Figure16. Thermal stress field of reinforced bridge piers (a: non-reinforcement concrete, b: reinforcement concrete)

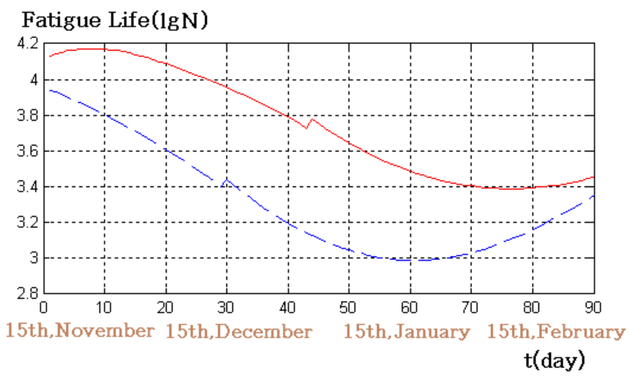

Figure 17. Fatigue life change of reinforced bridge piers (--: non-reinforcement concrete, -: reinforcement concrete)

 DOI: https://doi.org/10.30564/hsme.v1i1.1009

References

[1] Ma Y, Che Y, Gong J. Behavior of corrosion damaged circular reinforced concrete columns under cyclic loading[J]. Construction and Building Materials, 2012, 29: 548-556.
DOI: 10.1016/j.conbuildmat.2011.11.002

[2] Ma Y, Xiang Y, Wang L, et al. Fatigue life prediction for aging RC beams considering corrosive environments[J]. Engineering Structures, 2014, 79: 211-221.
DOI: org/10.1016/j.engstruct.2014.07.039

[3] Guo A, Li H, Ba X, et al. Experimental investigation on the cyclic performance of reinforced concrete piers with chloride-induced corrosion in marine environment[J]. Engineering Structures, 2015, 105: 1-11.
DOI: org/10.1016/j.engstruct.2015.09.031

[4] Yuan W, Guo A, Yuan W, et al. Experimental investigation on cyclic behavior of coastal bridge piers with non-uniform corrosion under biaxial quasi-static loads[J]. Construction and Building Materials, 2018, 190: 222-234.
DOI: org/10.1016/j.conbuildmat.2018.09.151

[5] Guo A, Yuan W, Li H, et al. Structural strength deterioration of coastal bridge piers considering non-uniform corrosion in marine environments[J]. Earthquake Engineering and Engineering Vibration, 2018, 17(2): 429-444.
DOI: org/10.1007/s11803-018-0451-z

[6] Li G, Lin J. Experimental research on improving surface quality of concrete pier[J]. Journal of Railway Engineering Society, 2005, 87: 53-57.

[7] Hamze Y. Concrete durability in harsh environmental conditions exposed to freeze thaw cycles[J]. Physics Procedia, 2014, 55: 265-270.
DOI: 10.1016/j.phpro.2014.07.038

[8] Kang F, Li J, Zhao S, et al. Structural health monitoring of concrete dams using long-term air temperature for thermal effect simulation[J]. Engineering Structures, 2019, 180: 642-653.
DOI: org/10.1016/j.engstruct.2018.11.065

[9] Ulf Ohlsson, Fracture mechanics analysis of concrete structures, Doctoral Thesis, Lulea University of Technology, 1995, 196-203.

[10] SolidWorks Cooperation, Documentation for SolidWorks2018, 2018.

[11] MathWorks Inc., Documentation for MATLAB 2018, 2018.

[12] ANSYS Inc., Release 19.0 Documentation for ANSYS, 2018.

DOI: https://doi.org/10.30564/hsme.v1i1.1009

BILINGUAL PUBLISHING CO.
Pioneer of Global Academics Since 1984

Hydro Science & Marine Engineering
https://ojs.bilpublishing.com/index.php/hsme

ARTICLE

Practice Study on Operation Evaluation and Limitation for Merchant Ships in Polar Water

Shifeng Ding[1] **Li Zhou**[1*] **Chenkang Zhong**[2] **Zhengrong Wang**[2]

1. School of Naval Architecture and Ocean Engineering, Jiangsu University of Science and Technology, Zhenjiang, 212003, China
2. Shanghai Rules and Research Institute, China Classification Society, Shanghai, 200135, China

ARTICLE INFO

Article history
Received: 29 July 2019
Accepted: 20 August 2019
Published Online: 31 October 2019

Keywords:
Polar Ship
Operational Risk Assessment
Ice Operation Limitation
Risk Analysis

ABSTRACT

All environmental hazards impact the safety of polar ships, especially polar merchant ship with light ice-class. In order to provide a systematic guidance to deal with any situation during polar operation, International Maritime Organization (IMO) raised mandatory requirements of "Polar Water Operation Manual"(PWOM) in Polar Code. This paper focuses on how to determinate operational evaluation and limitation for the PWOM, which is an important measure to avoid polar ships exceeding operational capability. Features of polar navigation are summarized based on the former polar navigation experience, and typical risk model is set up to describe the process of operation evaluation. The operational limitation is analyzed to indicate the actual capability and limitation as the ship encounters unexpected accidents in polar waters. In conclusion, the operation procedure is studied to give a detailed technical proposals for the whole polar operation, which is the main component of PWOM. The outcome may provide help for to arctic shipping of merchant ships.

1. Introduction

As arctic ice coverage decreases with global warming, more and more merchant ships want to use arctic shipping routes in summer [1, 2]. The arctic shipping has great value for reducing shipping cost, increasing shipping safety, saving energy and reducing emission. However, polar navigation is quite different from conventional one since it needs the maritime industry to be more cautious. International Maritime Safety Committee (IMO) ninety-fourth session formally adopted "International Code for Ship Operating in Polar Waters (Polar Code)" [3], and it came into effect on January 1, 2017. "Polar Water Operation Manual (PWOM)" is one of the main parts of Polar Code, which is a compulsive requirement from IMO. The PWOM explains ship operational limitation and operation procedure to captain and crew, and it is an important measure to guarantee the safety of polar shipping.

Polar navigation has additional hazards[4,5] besides conventional situation. In 2013's summer, a Chinese merchant ship named "Yongsheng" successfully sailed through arctic northeast channel[6], and it attracted more merchant ships to attempt the arctic navigation. As the IMO's Polar Code took effect on January 1, 2017, all polar merchant ships must prepare the PWOM[7-8], including ship's ca-

**Corresponding Author:*
Li Zhou,
School of Naval Architecture and Ocean Engineering, Jiangsu University of Science and Technology, Zhenjiang, 212003, China;
Email: zhouli209@hotmail.com

 DOI: https://doi.org/10.30564/hsme.v1i1.1082

pability and limitation, procedures for normal operation, special procedures for accident, measures for the use of icebreaker assistance etc. It is a realistic question to prepare the eligible PWOM for all shipping companies that want to attempt polar voyage.

This paper studies on the merchant ship's operational evaluation and limitation in polar water. The existing arctic navigation experience was summarized, including Xuelong ice-breaking research ship and Yongsheng ice-strengthened merchant ship. The operational evaluation method was studied based on the key factors which affected the safety of arctic navigation. A series of risk analysis models were set up to simulate the scenes during polar operation. Then the operational capacity and limitation was analyzed to reduce the risk level of polar operation when the ship encountered accident. As a conclusion, the operation procedure was established to direct the whole polar navigation process, which is the key to form PWOM. Eventually, the outcome was verified by the followed polar shipping voyages, and it was a technical basis for the implementation of the IMO's Polar Code.

2. The Features of Polar Navigation

The polar environmental condition is harsher than conventional waters, geographical location of the former is remote, and ecological environment is fragile [9]. Thus, the polar ships face higher risk level than conventional ships, and the situation also was varied with geographical location, air temperature and ice cover and other factors. The requirements of PWOM in Polar Code only include the targets, functional requirements and risk based operating procedures in Polar Code. However, it is necessary to develop a detailed technical method on how to prepare the qualified PWOM related to ship types, ice conditions and expected operating area.

The existing practical experience for ships was summarized, including Xuelong and Yongsheng (see figure1). The key steps were applied for polar navigation assessment, as shown in figure 2.

Figure 1. Polar navigation of Chinese ship

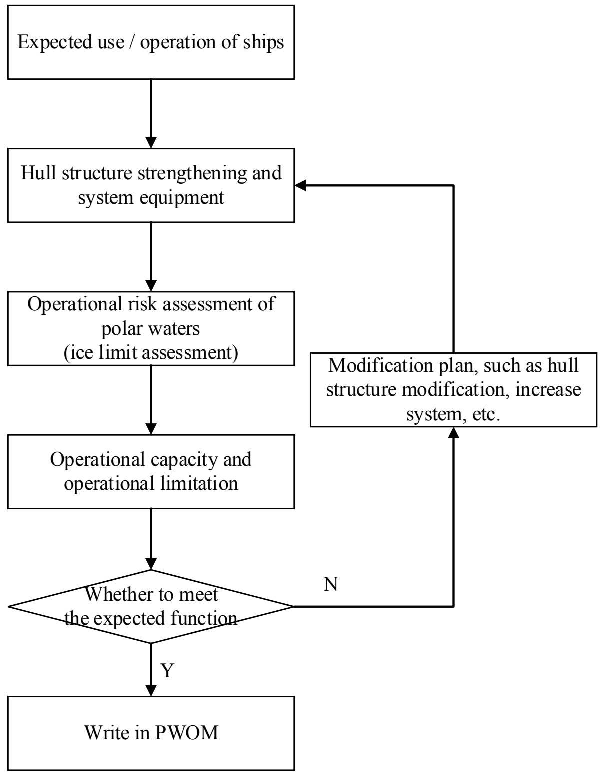

Figure 2. Key steps for polar navigation assessment

From Figure2, polar navigation was function oriented, which was distinguished from conventional navigation. The main features were presented as follow. The relationship was very close among operational measures, expected task and the ship's operational capability. The hull structure and system equipment was specially evaluated to be suit for the ice condition and low air temperature. All the hazards were studied to determinate the risk level during the polar navigation. The possible measures have been planned ahead to improve the safety when the ship encounter the unexpected polar environment.

In order to gain the qualified POWM, all features mentioned above should be fully considered to develop a method on operational evaluation and limitation. The method could be divided into three parts: how to carry out the operation evaluation, how to determinate the operational capacity and limitation, and what should be done when the ship exceeds its limitation. These issues will be studied further.

3. Operation Evaluation Method

The operational evaluation of polar ships and system equipment should be conducted to constitute the contents of the polar ship certificate. The intact operational evaluation is consisted of ice status, temperature, high latitudes and other hazards. There were four steps for the operation-

DOI: https://doi.org/10.30564/hsme.v1i1.1082

al evaluation process: identifying risk, formulating a risk model, assessing and determining risk acceptability, identifying existing or developing risk control alternatives.

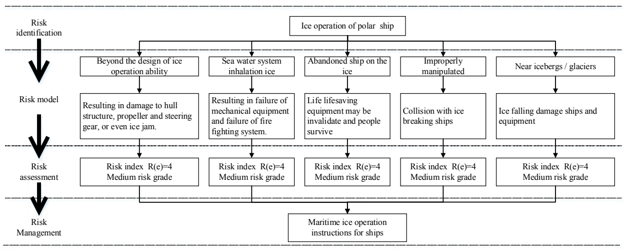

Figure 3. Risk analysis process for polar ship

The ice operation was taken as an example to illustrate the flowchart of risk analysis process as shown in Figure3. From figure 3, the operational evaluation was made up of a series of risk analysis processes. There were about 10 main sources of hazards listed in IMO's Polar Code, including sea ice, experiencing topside icing, low temperature, extended periods of darkness or daylight, high latitude, lack of accurate and complete hydrographic data and information, potential lack of ship crew experience, lack of suitable emergency response equipment, rapidly changing and severe weather conditions, sensitivity environment. All anticipated hazards should be analyzed to reduce their impact on polar ship and polar environment. Considering the expected hazards, several risk models were built respectively separated from the whole ship system. The risk assessment was analyzed to indicate the different risk level, and then some proper measures were studied according to severity of consequences.

4. Determination of the Operational Limitation

The polar operation of the merchant ship was limited by four main factors, including sea ice, low temperature, high latitude and ship's endurance. Sea ice may destroy the hull structure and trap ship, and it is a crucial factor for a merchant ship to choose the arctic route. Low temperature threats to the life-saving and fire-extinguishing systems, and it may also appeared in summer arctic water occasionally. High latitude affects the communication and navigation systems, which take a vital role in the safety of polar navigation. Ship's endurance directly affects the distance and time of whole polar voyage. All these factors should be studied.

4.1 Polar Operation against Sea Ice

The ship's ice operational capability is classified according to the ice class rule related to the nominal thickness of a single ice type [10]. This is idealized for ice conditions, which doesn't exist in reality. The actual ice condition is composed of various types of ice and its corresponding density, such as medium thickness of first year ice, old thick ice. However, the ice information received from weather forecast and ship observation is usually inconsistent with the ice-class. Thus, it is necessary to set up a relationship between ice information and ice class for a merchant ship.

In order to ensure the safety of ice operation, there are four assessment methods: Polar Operational Limit Assessment Risk Indexing System (POLARIS) provided by IACS, Arctic Ice Area Navigation System (AIRSS) provided by Canada, Arctic/Time System (Z/DS) provided by Canada and Ice Passport provided by Russia. All those methods could provide the empirical proposal about "going or not going" referring to the given ice condition.

In this paper, we mainly focus on the latest POLARIS. The ice condition is the decisive factor for choosing the ice class. First, operational time and area are chosen according to target task, and ice information is collected for the whole polar voyage. The operation risk index RIO is calculated referring to the worst ice conditions to determinate the suitable ice-class with formula(1)[7,8]. The ship is capable to operate in the ice water when the RIO is larger than zero, vice versa. Additionally, the RIO value may plus 10 with the escort of icebreaker.

$$RIO = (C_1 \times RIV_1) + (C_2 \times RIV_2) + (C_3 \times RIV_3) + \ldots (C_n \times RIV_n) \quad (1)$$

Where: $C_1 \ldots C_n$ are the concentrations of ice types within the ice regime; $RIV_1 \ldots RIV_n$ are the corresponding Risk Index Values for each ice type.

The calculated RIO could indicate the ice operational proposal based on the encountered ice condition. Then some proactive measures could be adopt in advance to avoid the severe ice condition exceeding the ship's ice operational limitation, such as changing navigation time or route, requesting escort of ice-breaker.

4.2 Effect of Low Temperature

All ships with the lowest daily average temperature (LMDLT) below -10 degree are required to consider the operation capacity and limitation of low temperature according to the requirements of IMO's Polar Code. The low temperature may freeze fire-fighting water and impact function of life-saving system. It is a great threat to the ship in emergency. The limitation of low temperature is related to the ship's service temperature (PST), which is lower than the LMDLT-10 degree at least. The definition of LMDLT is shown in Figure4.

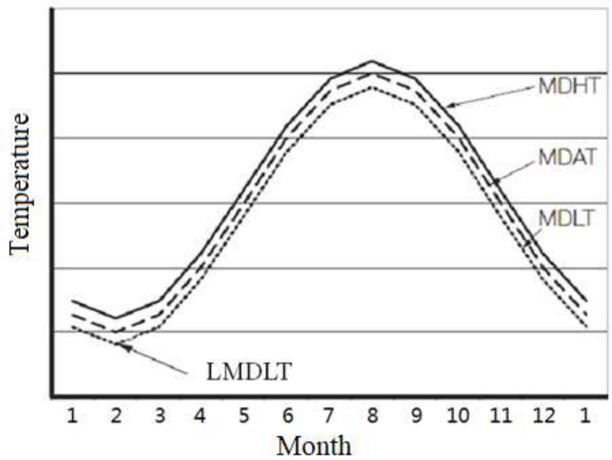

Figure 4. The temperature definition [7]

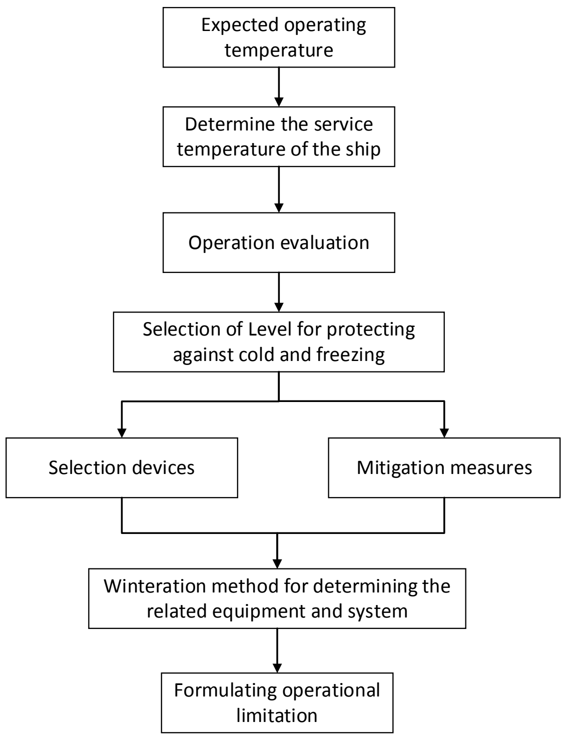

Figure 5. Evaluation process on operational limitation of low temperature

The evaluation process on how to determinate the low temperature limitation is summarized as Figure 5. The lowest temperature in arctic waters is about 0 degree during July to October referring to the existing meteorological data. It is unnecessary to consider the operational limitation of low temperature for a merchant according to the requirement of Polar Code. However, the freezing phenomenon is still possible during the arctic summer voyages. It is wise to adopt some useful de-icing measures, such as hammer, shovel, which could prevent key systems and devices (e.g. life-saving system, escape route) from icing.

4.3 High Latitude

The electromagnetic environment is complex in high latitude area, which impacts the normal use of communication and navigation equipment during polar navigation. According to the existing experience, direction force of the magnetic compass is too weak and unstable at more than 60 degree latitude, and the signal of GMDSS and GPS is unstable at more than 80 degree latitude. That may pose a great risk to polar navigation. It is necessary to equip the reliable communication and navigation equipment for polar voyage at high latitude.

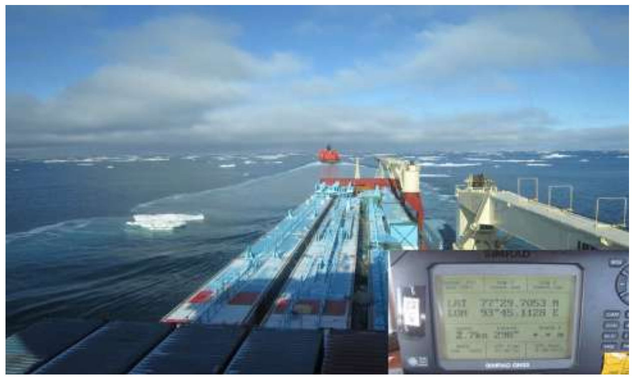

Figure 6. Navigation of merchant ship at high latitude

In general, the highest latitude of a merchant ship's summer arctic route was about 77 degree (see Figure 6). The magnetic compass and gyrocompass are uncertain at that high latitude. Nonetheless, the INMARSAT system and GPS system are available for communication and positioning. The iridium satellite phone would also provide an ideal communication equipment at high latitude. Therefore, all communication and navigation equipment should be examined carefully to ensure applicability at the expected high latitude. It is the guarantee of the safety for polar operation.

4.4 Ship's Endurance

The planned ship velocity [11-15] is influenced by many unexpected factors, such as severe ice condition, unexpected low temperature, dense fog, lack of the escort of icebreakers. It is advisable to plan the ship's voyage carefully to ensure sufficient ship's endurance in polar waters.

The limitation of ship's endurance depends on two factors. One is the storage of fuel, food and fresh water, and the other is the disposal or storage capability of pollutant. Thus, the captain must take management and control of endurance capability into consideration during the voyage plan in polar waters. According to the existing experience, it usually need about 10 days for a conventional merchant ship to cross the northeast passage in summer. The en-

  DOI: https://doi.org/10.30564/hsme.v1i1.1082

durance of polar ship should be no less than 1.2×10 days =12days.

5. Operation Procedures

There is no absolute safety in polar navigation, because the unexpected situations may occurr occasionally. Although the ship has been evaluated carefully, the operation procedures must be studied based on risk assessment including conventional operation procedures for normal working scenario and emergency operation procedures for unexpected accident scenario. The process of making the operational procedures is summarized in Figure7.

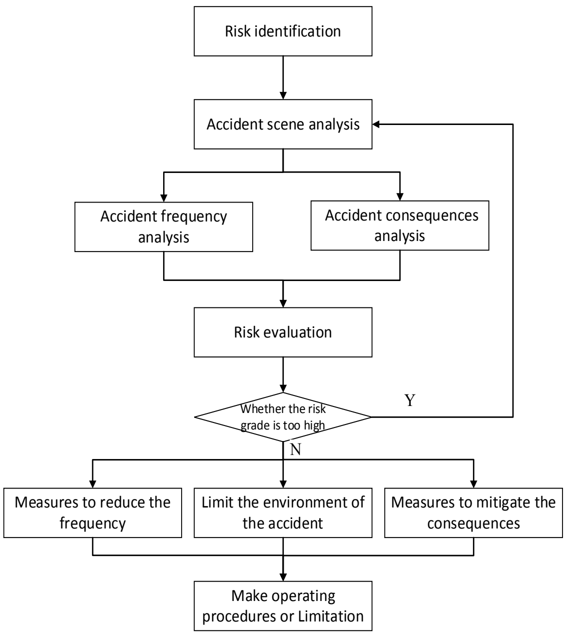

Figure 7. Process of making the operational procedures

The ice operation procedure is taken as an example for a merchant ship with IA ice class. The IA ice class is sufficient for the light first-year ice during summer arctic navigation. But sometimes the thick multiyear ice from the high latitude area may appear at the planed voyage, which is beyond the ice operational limitation of IA ice-class. The risk level could be evaluated according to the dangerous scenario with quantitative risk assessment method (QRA). Some appropriate measures could be adopted in case of the extreme risk level, which includes modifying the voyage plan, strengthening observation of ice condition to reduce the occurrence probability of encountering severe ice condition, optimizing structure to avoid the damage caused by ice impact, requesting the escort of ice-breaker. Eventually, the measures referring to all expected ice conditions should be concluded in the ice operation procedure. The correct operational measures could be chosen from ice operation procedure for the different ice conditions during polar voyage.

6. Practical verification of Arctic navigation

The present method for merchant ship's operational evaluation and limitation was vilified by bi-directional navigation through Northeast Passage of Yongsheng in 2015. Yongsheng ship departed from Dalian port at 8th July 2015, and sailed to north Europe through the arctic Northeast Passage. Then it returned to China at 3rd October after 55 days and nearly 20 thousand nautical miles. That polar voyage plan had a long time period with severe ice condition, which pioneered the first time that China's merchant ships passed through the Arctic Northeast Passage from Europe to China.

At the voyage planning stage, ice condition is the key to choose the ship with ice-class. The worst ice conditions during that polar voyage was collected as Figure8.

Figure 8. Statistical/expected ice information processing

The calculated RIO values referring to ice-classes were listed in table 1 with POLARIS method.

Table 1. RIO for different ice class ships

Ice Class	RIO Value	Result
PC5	21	P
PC6	21	P
PC7	12	P
B1*/IA Supper	12	P
B1/IA	3	P
B2/IB	-6	N
B3/IC	-6	N

Note: P means the ship is able to ice operate; N means the ship can't ice operate.

The results shows that B1 ice-class is necessary for that specified voyage planning without additional measures. However, ice class of B2 and B3 also could be chosen with especial icebreaker escort. Finally, Yongsheng with ice-class B1 was chosen.

The POLARIS method is also meaningful for ships entering the ice waters. When captain receives the ice information on the route ahead, the RIO value is used to decide the next step of the navigation strategy. During the ice operation in polar waters, the next ice condition in front of Yongsheng was 3/10 medium first-year ice, 6/10 thin first-year ice, 1/10 open water.

 DOI: https://doi.org/10.30564/hsme.v1i1.1082

The ice information was analyzed with EGG Code as Figure9.

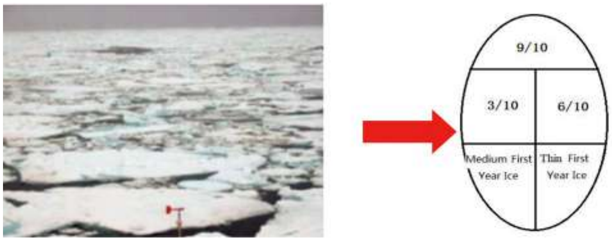

Figure 9. Real-time ice information processing

The calculated RIO value with POLARIS was 6, it illustrated that the ship could sail ahead in the expected ice condition. According to the above method, PWOM of "Yongsheng" ship was formulated based on risk analysis considering all the hazards and corresponding control measures. It played a vital role during the actual arctic shipping and reduced the influence to mariners, ship structure, goods and polar environment.

7. Conclusion

The shipping industry is paying more and more attention to the arctic shipping because of great commercial value and economic benefits. It is very important to study operational evaluation and limitation of merchant ship, because safety is the key for polar navigation. This paper summarizes the previous experience on polar navigation, and presents a method on operational evaluation and limitation. Three practical questions are solved including how to carry out the operation evaluation, how to determinate the operational capacity and limitation, and how to do when the ship exceeds its limitation. The outcome has been used in Chinese arctic shipping since 2015, which has the practical significance of engineering application and shipping guidance.

Funding

This research was funded by the National Natural Science Foundation of China, grant number 51809124, 51911530156; Natural Science Foundation of Jiangsu Province of China, grant number BK20170576; Natural Science Foundation of the Higher Education Institutions of Jiangsu Province of China, grant number 17KJB580006; State Key Laboratory of Ocean Engineering (Shanghai Jiao Tong University), grant number 1704 and 1807.

References

[1] Mulherin D N. The Northern Sea Route - its development and evolving state of operations in the 1990s[J]. philadelphia:the American society forting and materials, 1996: 1-2.

[2] L Eder, P Andrewsspeed, A Korzhubaev. Russia's evolving energy policy for its eastern regions, and implications for oil and gas cooperation between Russia and China[J]. Journal of World Energy Law & Business, 2009, 2(3): 219-242.

[3] Committee I M O M S. International code for ships operating in polar waters (Polar codes): resolution MSC.386(94) [M]. International Maritime Organization, 2016.

[4] Shen Quan. Seeing the risk of polar navigation and the development trend of icebreaker from the perspective of "Xue Long" rescuing Russian ships. [J]. Navigation, 2014 (2): 14-18.

[5] Fu Shanshan, Zhang Di, Sang Lingzhi, etc.. Application of flexible engineering theory in risk prevention and control of polar ships navigation [J]. Polar Research, 2016, 28 (2): 250-256.

[6] Wang Luo, Zhao Yue, Liu Jianming, etc.. The Northeast navigation channel of Chinese ship's first voyage and its prospect [J]. Polar Research, 2014 (2): 276-284.

[7] CCS. Guidelines for polar ship[S]. 2015.

[8] CCS. Guidelines for polar water operational manual[S]. 2016.

[9] Ying Junjun, Feng Zhengping, Liu Lele, etc.. The analysis of the polar sea ice environment [J]. Ship, 2017, 28 (2): 10-18.

[10] Shifeng Ding, Li Zhou, Chenkang Zhong, etc.. A Structural Analysis Procedure Combining Linear and Nonlinear FE Methods for Polar Ship[C]. Proceedings of the Twenty-ninth (2019) International Ocean and Polar Engineering Conference Honolulu, Hawaii, USA, June 16-21, 2019.

[11] E M Gramuzov, N A Kuzmin, M Y Sandakov, etc.. The influence of ice conditions when creating the hull for ice navigation[J]. 2019, 1177(1): 1-7.

[12] R.W. Liu, Y.Z. Xue, X.K. Lu, etc.. Simulation of ship navigation in ice rubble based on peridynamics[J]. Ocean Engineering, 2018, 14(8): 286-298.

[13] Jian Hu, Li Zhou. Experimental and numerical study on ice resistance for icebreaking vessels[J]. International Journal of Naval Architecture and Ocean Engineering, 2015, 7: 626-639.

[14] Jian Hu, Li Zhou. Further study on level ice resistance and channel resistance for an icebreaking vessel[J]. International Journal of Naval Architecture and Ocean Engineering, 2016, 8: 169-176.

[15] Li Zhou, Zhenju Chuang, Chunyan Ji. Ice forces acting on towed ship in level ice with straight drift. Part I:Analysis of model test data[J]. International Journal of Naval Architecture and Ocean Engineering, 2018, 10: 60-68.

  DOI: https://doi.org/10.30564/hsme.v1i1.1082

BILINGUAL PUBLISHING CO.
Pioneer of Global Academics Since 1984

Hydro Science & Marine Engineering
https://ojs.bilpublishing.com/index.php/hsme

ARTICLE

Design of Flood Drainage in Golgohar Iron Ore Mine#3

Saeid Maknouni Gilani*

Shiraz University and Golgohar Mining and Industry Co., Km 50 Shiraz road, Sirjan, Kerman, Iran

ARTICLE INFO

Article history
Received: 26 September 2019
Accepted: 21 October 2019
Published Online: 31 October 2019

Keywords:
Golgohar
Flood
Watershed
Mine
Drainage
Curve Number

ABSTRACT

The iron ore minerals reservoir of Golgohar Mine#3 is more than 660 million tons. It is the biggest in Iran and rate of ore extraction is more than 15 million tons per year. The pit takes place on the way of runoff pathway of this watershed and it needs an especial strategy for conserving the pit mine during next imminent floods. The area of Mine# 3 watershed is 20785700 square meters and its general slope in its topography map is 0.59 percent; then initial scheming indicates it can causes a great deal of problems for mining operation n the next floods; particularly, the pit is located into degree 4th sub branch of a main ephemeral river. For this purpose, the Soil Conservation Service Curve Number (SCS) method was employed to estimate intervals period of next floods based on the magnitude, the intensity and the duration of precipitation events data. Conceptual design of runoff drainage of the watershed was designed to lead the flood to a better pathway location. The Mine#3 overburden deposition occupies a huge area on the watershed; and it has been considered and redesigned in terms of size, form, dimensions and location to manage as a physical obstacle against next floods. Hydraulic calculations were applied for designing two essential open channels which can preserve the pit.

1. Introduction

The Golgohar Iron Ore Mine (GIOM) is including six major iron ore mines. The total iron mineral reservoir of these mines is more than 1.3 billion tons, including mainly magnetite iron ore. Currently, five mines are being extracted. Economical geology study in Mine#3 shows the mine, with 660 million tons, is the most principal iron ore reservoir in Iran. Extraction operation of this mine has started in the northern half of the mine from 2004. Mine extraction method has selected open pit.

2. The Study Area

Iran's largest iron ore deposits take place in the GIOM [17,18]. The mine is located 950 km south of Tehran in Kerman province about 55 km southwest of Sirjan city (see Figure 1). The study area, the GIOM, is located in the middle south of Iran (55° 16′ to 55° 20′ E and 29° 05′ to 29° 06′ N) shown in Figure 1 [17,18]. This area has a unique geological history in the Middle East. Many scientists believe that in the south of the Paleotethys Ocean, the block of Central Iran during the movement toward the North has met the block of Eurasia in late Permian [6] Almost at the same time, the Neotethys Ocean appeared in the South between the Arabian and the Central Iran block. The best witness to this event is upper Triassic to Jurassic sediments (Ophiolite) that are presently between

**Corresponding Author:*
Maknooni Gilani,
Shiraz University and Golgohar Mining and Industry Co., Km 50 Shiraz road, Sirjan, Kerman, Iran;
Email: maknooni_s@shirazu.ac.ir; maknouni_sa@golgohar.com

these two blocks in the southern part of Iran [6,9]. After that, the trend of opening of Neotethys has been reversed and the subduction of ocean crust of Arabic block under the Iran block started [9]).Then, an elongated zone consisting of magma and igneous rocks was created parallel to the Neotethys Ocean, as the Sanandaj-Sirjan structural zone was named after the names of the cities located in the beginning and the end of the zone in Iran. About the time of the closing of Neotethys ocean, some scientists believe the closing occurred in late Cretaceous to Paleocene 6,15], some determine it late Oligocene [1] and even some suggest Miocene [5,10,12].

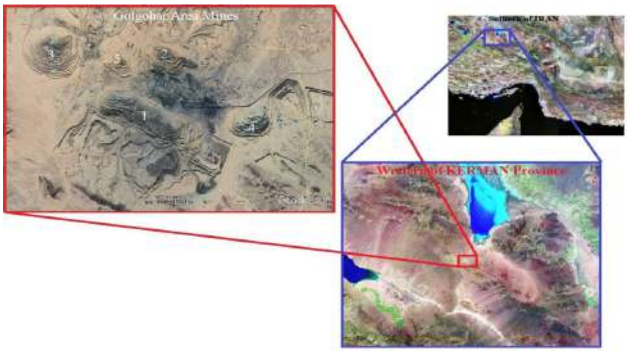

Figure 1. The location of the GIOM

Tectonic Sanandaj-Sirjan zone has many folded igneous and metamorphic rocks accompanied by lots of reversed or normal faults which are formed in an extensive period [8]. The Calc-alkaline and volcanic rocks prove that this zone was an active continental margin in Mesozoic. A kind of magmatic arc is found in Sirjan and many other areas in the zone of Sanandaj-Sirjan [2,3,4,7,11,13,14,16], .

GIOM is located in the margin of the central desert of Iran in the zone of Sanandaj-Sirjan and is bounded by some salt pan in the north and south. Few local, medium height mountains are also seen in the north and south of the area [17,18].

The structural zone of the area is the most active tectonic zone in Iran and has passed the Cenozoic magmatic and metamorphic phases. The GIOM is placed in the Paleozoic metamorphic rocks as the oldest formations in this area termed as Golgohar Metamorphic Complex (GMC) formation, which includes five hard rock units: (1) serpentinized ultramafic and metamorphic rocks, (2) dolomitic marbles to Calcific Marbles, (3) Mica schist some gneiss and amphibolite, (4) Gneiss and (5) an alternate of marbles, gneiss, mica schist, amphibolite, schist and black quartzite on the gneiss [14]. Units one and two are not exposed in the GIOM area. The complex has no distinct lithological pattern in depth or surface. The complex consists of six ore field sets [17,18].

The topography of the study area of the five rain catchments surrounding the GIOM, i.e. the Chahderaz (CH), the Qatarbaneh (QA), the Ein-ol-Baghar (EB), the Kheyrabad (KH), and the Mine (MI) rain catchment areas is shown in Figure1. The PW-A15 is located nearby the boundaries of the CH, EB and MI catchments. Long period average annual precipitation of the area is 148 mm, which mainly happens in the winter. The potential evaporation is reported to be more than 2800 mm in a year. There is no eternal river in a radius of 200 km of the area. The climate of the area is semiarid to arid with cold winters and warm summers [17,18].

The SSZ structural geology state is formed as a strip with a width of 150 to 200 km parallel to the last remnants of Neotethys to the Zagros Mountains suture. The Closing of this paleo-ocean was coincided the crust subduction of the Neotethys plate beneath the central Iran plate. At the same time, volcanic lava erupted along the SSZ. The SSZ structural geology state is known as a poly-phase deformed zone. The age of the Neotethys closing is not definitely found out. The first group of scientists says it happened in the late Cretaceous to Paleocene [6,15]. But others found it the late Oligocene [1] and some of them discovered it the Miocene [5,10,12].

So far, different theories about the SSZ creation have been presented. Many believes that this zone is a product of the imbricate slice of the ocean crust along with the metamorphic agglomerate in the green schist faces. Some other geologists state the SSZ is as a part of the Central Iran [6,15], which has a subduction toward the north [6,9]. Another theory says the existence of this zone was a micro-continental plate into the paleo-ocean [1]. And some others demonstrate the SSZ is a part of the Arabian plate which was appended to the Eurasian plate as a rifted plate [1]. The recent theory is rejected due to disaffiliation of the lithology.

The lithology of the GMC was generally studied [17,18] (Figure 2). Many parts of the study area were covered by hard formation members of GMC formation [17,18]. The GMC is made of Neotethys sediments formation of Paleozoic (Figure2). But the age of metamorphism in GMC formation is calculated based on the Argon isotopic studies Jurassic [17,18]. In terms of geomorphology, the GIOM takes place on the flat plateau [17,18] (Figure 3). The Lithology of some mountains of the study area is made from carbonate part of the GMC. Alluvial plain in the GIOM is 1730 meters high in average. There are three salt pans in study area, the More and the Meydan-Gel salt pans in the south the Kheyrabad in the north.

DOI: https://doi.org/10.30564/hsme.v1i1.1255

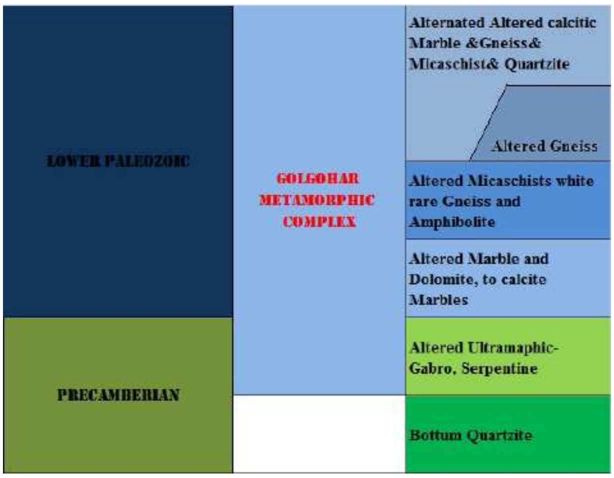

Figure 2. The GMC stratigraphy

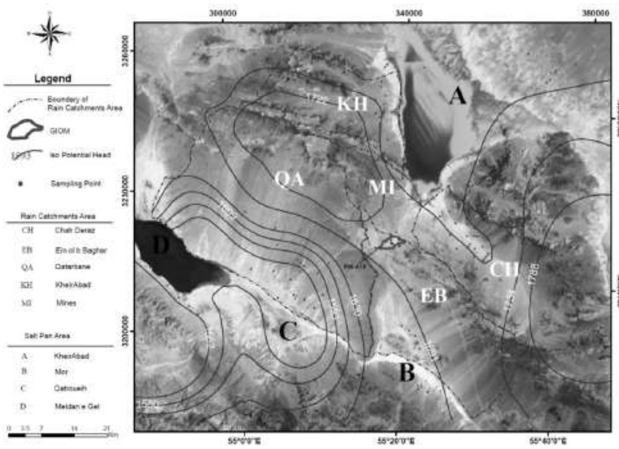

Figure 3. The rain catchment area, salt pans and topography map around of the GIOM

3. Definition of problem

There are numerous problems in mining. Some of them can be due to existence of water. Primarily, it would be better to mention a few of these problems:

(1) Groundwater seepage increasing

(2) Flood damage

(3) Need to increase dynamic drawdown of mine groundwater

(4) Necessity to a tailing dam to collect wastewater of factories (and mine wastewater too)

(5) Incorrect locating of mine deposits (waste, ore, overburden and etc.) in mine rain catchment area

Many techniques have to be applied to solve each of these problems.

In 1992, it precipitated 130 millimeter in the area during three days. The 3 deepest benches of the Mine#1 were under-watered due to flood flow that had started from upstream of the mine. Its subsequent economical detriment was perceptible. In 2017 another flood occurred in this area which affected all of the five mines. This second flood took place after a 170 mm precipitation, that it caused more structure damage of the mines and facilities of them. This paper tries to presents a manner to restrain future floods in a watershed.

4. Materials and Methods

At first, boundaries of the rain catchment areas were determined around the GIOM. For this purpose, *ArcView* GIS software was applied. Then the output of it was transferred to *Gemcom* software which uses in mining operation. The physiography characteristics of the watersheds were also obtained using geological and topographic parameters using topography maps of the area. Precipitation data was obtained from meteorological station which located into the GIOM area. A synoptic meteorological station in the GIOM region was established in 2006. But before then, for more than 20 years, the meteorological data were gathered using another old climatological station where was nearby the same station. Using these digits, distribution of precipitation statistics in these mines was analyzed. The period time of flood was calculated in the area using these 2 softwares: *Distrib 2.13* and *Smada 6.43*. Using the physiological characteristics of the rain catchment area, which was measured on topography map, the hydraulic coefficients of the field were obtained for estimating the runoff. The unit hydrograph of the watershed was calculated applying *Smada 6.43*. Methodical analyzes of the flood characteristics of the selected watershed were calculated for different periods of the floods flow. It was decided that the Mine#3 designing should be protected effects of the 200 year flood. Knowing the hydrological characteristics of the 200 year flood, the location of flood outlet in the watershed and the overburden deposition of the mine was determined. Also, some essential specifications of the watershed are deliberated for hydraulic designing of the flood drainage channels. For this purpose, hydraulic calculations of open channel river were applied.

5. Results

The rain catchment areas of the GIOM area were recognized using the 1/10000 GIOM topography map. There are five following Rain catchment areas which encircle the six mines:

(1) Rain catchment area No.1 or Chahderaz

(2) Rain catchment area No.2 or Ein-ol-Baghar

(3) Rain catchment area No.3 or Ghatar-Bane

(4) Rain catchment area No.4 or Kheyrabad

(5) Rain catchment area No.5 or Mines

These watersheds are shown in Figure1. The flood of the No.2 and 3 rain catchment areas transfer over the south of the study area towards Mor and Meydan-Gel salt pans. The flood of No.1, 4 and 5 rain catchment areas pour over towards the Kheyrabad salt pan in the North.

Above classification was re-checked. The *ArcView* software researches focuses in the study area where includes all six mines and their industrial units:

(1) Factory watershed
(2) Mine#1 watershed
(3) Mine#2 watershed
(4) Mine#3 watershed
(5) Northern watershed
(6)Tailing Dam#1 watershed
(7) Tailing Dam#2 watershed
(8)Mine#6 watershed

Only the two last watersheds pour over the Ein-ol-Baghar rain catchment area, and the rest of them are geographically the portions of the Ghatar-Bane rain catchment area. This article focuses only on Mine#3 watershed.

5.1 Physical Properties of the Mine#3 Watershed

The area of the Mine#3 watershed is 20785700 square meters. This watershed is located in the west of the Mine#1 watershed. The outlet of these watersheds joins together in the South of them. The watershed runoff pours toward the South of the Mine#3 watershed where locates the Southeast of Mine#1. This property of the watershed hazardously affects technical activities of these mines during floods. Because the runoff of floods can pass through the pits of the Mine#3 and 1 before they pour over the Ghatar-Bane rain catchment area basin [17,18].

The area of permeable part of this watershed is 18312800 square meters, and the non-permeable part is 2472900 square meters. The perimeter is 18250 m. Length of the watershed (based on the longest river) is 7600 meters. Other descriptive physical factors of this watershed determined: elongated watershed with 0.359 the shape factor, which indicates a high range and dangerous hydrograph for the facility located on it. The Gravelius coefficient is 1.121 which indicates a low deviation from the circle. Its elongation ratio is 0.677, which is a low rate. The length of rectangle is 4755.9 m and the width of it is 4370.5 m. The mean slope of watershed is calculated 0.59% using contour lines method. Slope direction in the west side of watershed is from the West to the East. But dominant slope direction of this watershed is from the North to the South.

Concentration time of the watershed was calculated using 6 below equations *Izzard, Kerby, Kirpich, Kinematic, Bransby-Williams* and *Federal Aviation Agency*. The average value of them for the concentration time is 237.7 minutes.

5.2 Distribution of Precipitation Statistics

The GIOM meteorological center is located 1 km far from the watershed. This center has proper long-term precipitation data. The 32-year precipitation data of this center was entered to a PC to run on *Distrib 2.13* software. Flood routing was performed by probabilistic method of location of *Weibull* data and distribution function of *Log Pearson type III*.

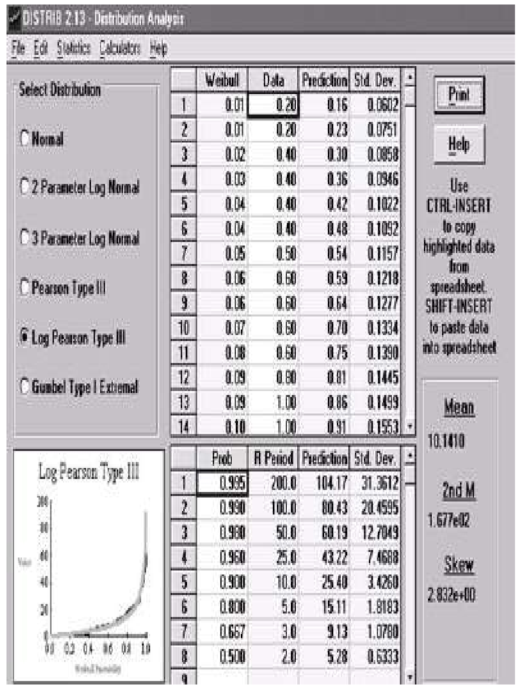

Figure 4. Using the *Distrib 2.13* software to recognize distribution and prediction of precipitation in Mine#3

The reason for choosing this distribution function in spite of its high standard deviation was that the *Log Pearson Type III* distribution function assessed the highest precipitation height and made the most realistic estimation of a 200 year flood of the mine against these five other distribution functions: *2 Parameters Log Normal, 3 Parameter Log Normal, Gamble, Gamble Type I External* and *Pearson Type III* (Figure4). Then, for this temperamental river, the highest precipitation height is preferred.

Table 1. Distribution of precipitation amount with different probability and return periods

Standard Deviation	Precipitation (mm)	Period (year)	Probability
31.36	104.17	200	0.955
20.46	80.43	100	0.99

  DOI: https://doi.org/10.30564/hsme.v1i1.1255

12.71	60.19	50	0.98
7.46	43.22	25	0.96
3.42	25.4	10	0.9
1.82	15.11	5	0.8
1.08	9.13	3	0.667
0.63	5.28	2	0.5

Accordingly, the probability of occurrence and height of precipitation runoff in the watershed with different periods are estimated in Table 1. The baseline of flood calculations for the project was assumed to be at least 200 years. Therefore, in future calculations, flood routing was performed for a precipitation of 174.14 mm.

Table 2. Distribution of precipitation intensity with different probability and return periods

Standard Deviation	Precipitation Intensity (mm/hour)	Period (year)	Probability
0.29	3.23	200	0.995
0.25	2.88	100	0.99
0.21	2.53	50	0.98
0.17	2.20	25	0.96
0.12	1.76	10	0.90
0.08	1.44	5	0.80
0.6	1.19	3	0.67
0.4	0.97	2	0.50

According to the GIOM precipitation records, this is equivalent to the 60-hour precipitation that occurred on January 19, 1992, that caused a $ 4 million damages to the mine, plants and their facilities.

Precipitation distribution was also considered in this process. In this estimation, the two-parameter log-normal distribution was used, that has the highest estimation intensity among 200-year-old period. The results of this estimation are presented in Table 2. Accordingly, the highest precipitation intensity with a 200-year period is 3.23 millimeter in hour.

Precipitation duration was also analyzed by above method and software; the results are presented in Table 3.

Table 3. Distribution of precipitation duration with different probability and return periods

Standard Deviation	Precipitation Duration (hour)	Period (year)	Probability
15.4	54.81	200	0.995
10.4	43.44	100	0.99
6.7	33.56	50	0.98
4.1	25.06	25	0.96
2.0	15.79	10	0.90
1.1	10.12	5	0.80
0.7	6.62	3	0.67
0.4	4.19	2	0.50

Therefore, the duration of flooding of a 200 year period is calculated 54.81 hours.

5.3 Watershed Runoff

In addition to using a cylindrical precipitation gauge, an automatic precipitation gauge was also installed at the GIOM meteorological station to calculate the runoff and to determine the watershed unit hydrograph.

Due to the lack of any hydrometric device in the river of the watershed there is not hydrography data during the flood, then the conventional Curve Number (CN) method was applied to estimate the surface runoff volume of the watershed and to obtain the unite hydrograph. The runoff CN is usually an empirical parameter which applied for flood or infiltration predicting from precipitation. The CN method was established by the USDA Natural Resources Conservation Service, and was previously called the Soil Conservation Service or SCS , the number is still commonly recognized as a "SCS runoff CN" in the hydrological studies. The CN is extensively applied in new studies too and is a proper method for deceiving a rough quantity of flood in each study area. According to the type of soil and the green cover quality, the CN value of the Mine#3 watershed was considered 70. Then, the precipitation statistics of one of the major floods in the watershed were calculated, that occurred in 1992, and was plotted using the above CN method (Figure 5).

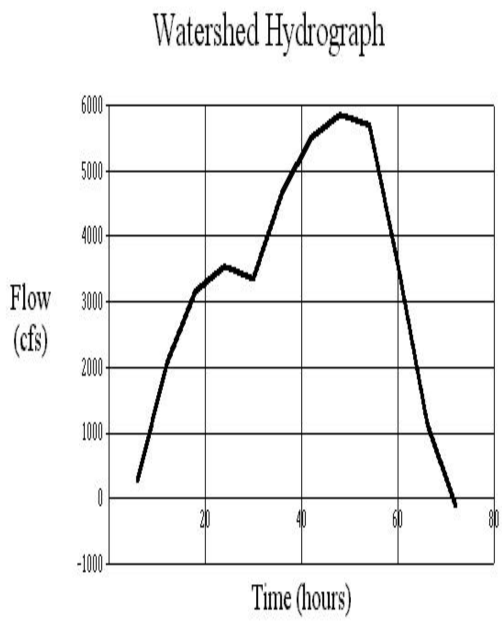

Figure 5. The hydrograph of Mine#3 watershed

Flood routing was performed applying *Smada 6.43* software using unit hydrograph of watershed. In this way, the flood hydrograph in the watershed was obtained by extending of the existing unit hydrograph (Figure3). Then, the 200-year flood peak discharge was calculated. The discharge of flood is 5206 cubic feet per second (147 cubic meters per second).

5.4 Flood Discharge Location

Determining of a deposit locating for flood is one of the major problems for the GIOM due to the following complications:

(1) The study area is factually a wide savannah; therefore, there is no bulky reservoir for flood accumulation.

(2) The pit Mine#3 takes place at the southern end of the watershed. The watershed flood should not be aggressing towards the pit, but its topography makes it flowing toward.

(3) The cost of tailing dam construction for this purpose is enormous.

(4) The Mine#1 is in the east of the Mine#3 watershed and the western heights overlooking Mine#3 restricts flood outlet of watershed (Figure 7).

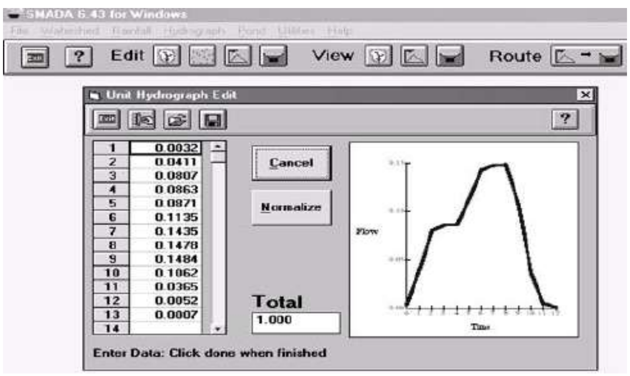

Figure 6. The unit hydrograph of the watershed using *Smada 6.43* software

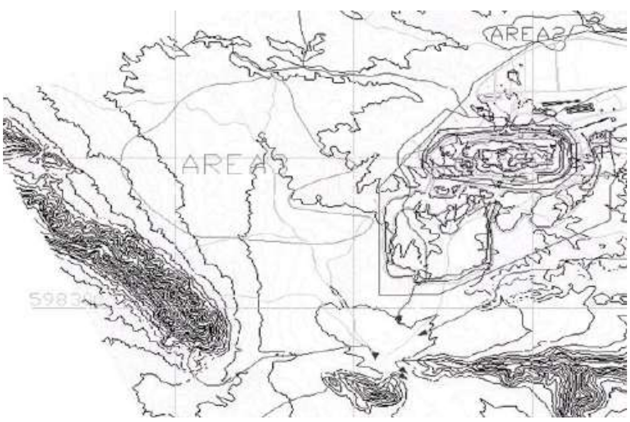

Figure 7. Topography map of Mine#3, watershed Mine#1 and these catchment outlet by *Gemcom 4.0* Software

After further field studies and investigates on the topographic maps of the area, it was decided that the flood of this watershed would diverge in two branches of river in the East and the West. From an environmental point of view, although this will be accompanied by a change in the natural path of the flood in the Northern half of the watershed, but it seems the existing technical and structural problems leave no other way to avoid it.

5.5 Channel Specifications

According to the flood characteristics of the watershed, the channel characteristics were calculated through open channel hydraulic calculations and river engineering references:

(1) Confidence factor: 1.80

(2) Wide of channel: 30 meters,

(3) Channel depth: 4 meters,

(4) Channel slope: 0.21%

(5) Section of channel: trapezoidal

(6) Channel slope is 1:2 or 26.58^{o}

(7) The length of the main channel: 3650 meters

(8) Channel width : 14 meters

(9) Area of channel surface: 96 square meters

(10) The wet-channel environment: 33.88 m

(11) The hydraulic radius of the channel: 2.83 meters

(12) Water velocity in channel: 2.78 meter per second

(13) Maximum water discharge: 266 cubic meters per second

Accompany with the main channel designing, as shown in Figure 8, a hydraulic gabion wall is need to restricted flood water into the channel. And a smaller channel is designed in the East of the Mine#3 to keep away the water from the pit. The final drainage design within the Mine#3 watershed was prepared using the *Gemcom* software (Figure 8).

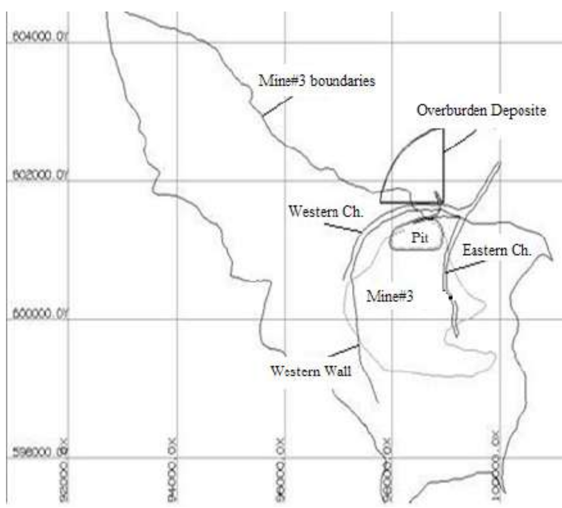

Figure 8. The schematic flood drainage design for the Mine#3

DOI: https://doi.org/10.30564/hsme.v1i1.1255

6. Conclusion

(1) Due to the location of the Mine # 3 on the way to the watershed river, next flooding events is inevitable.

(2) The special channel construction is necessary to gather the flood by two channels and a hydraulic wall..

(3) Finally, overburden deposit and facility location of Mine#3 was redesigned with hydrological and flood control perspectives.

Referrences

[1] Agard P, Omrani J, Jolivet L, Mouthereau F. Convergence history across Zagros (Iran): constraints from collisional and earlier deformation. International Journal of Earth Sciences, 2005, 94: 401-419.

[2] Alric G, Virlogeux D. Pétrographie et géochimie des roches métamorphiques et magmatiques de la région de Deh Bid-Bavanat, Chaîne de Sanandaj–Sirjan, Iran. Thése 3éme cycle, Université Scientifique et Médicale de Grenoble. France, 1977: 316.

[3] Azizi H, Jahangiri A. Cretaceous subduction-related volcanism in the northern Sanandaj-Sirjan Zone, Iran. Journal of Geodynamics, 2008, 45: 178-190.

[4] Babaie HA, Ghazi AM, Babaei A, La Tour TE, Hasanipak AA. Geochemistry of arc volcanic rocks of the Zagros Crush Zone, Neyriz, Iran. Journal of Asian Earth Science, 2001, 19: 61-76.

[5] Berberian F, Berberian M. Tectono-plutonic episodes in Iran. In: Gupta HK, Delany FM (eds.) Zagros, Hindukosh, Himalaya geodynamic evolution. American Geophysical Union Washington, 1981, 5-32.
DOI: 10.1029/GD003p0005

[6] Berberian M, King GCP. Towards a paleogeography and tectonic evolution of Iran. Can. J. Earth Sciences, 1981, 18: 210-265

[7] Berberian M, Nogol M . Preliminary explanation text of the geology of Deh Sard and Khabr maps with some remarks on the metamorphic complexes and the tectonics of the area (two geological maps, 1/100000 from the Hajiabad quadrangle map). Geological Survey of Iran. internal report 1-60, 1974.

[8] Braud J. Geological map of Kermanshah 1/250000 scale. Geological Survey of Iran, 1978.

[9] Davoudzadeh M, Soffel HC, Schmidt K. On the rotation of the Central-East Iran microplate. N Jb Geol Palaont Mh, 1981, 3: 180-192.

[10] Dewey JF, Pitman WC, Ryan WBF, Bonnin J. Plate tectonics and the evolution of the Alpine system. Geological Society of America Bulletin, 1973, 84: 3137-3180.

[11] Dimitrijevic MD. Geology of Kerman Region. Geological Survey of Iran, 1973, 72: 52-334.

[12] Forster H. Continental drift in Iran in relation to the Afar structures. In: Pilger A, Rosler A (eds), Afar between continental and oceanic rifting (VII). Schweizerbatsche Varlagsbuchhandlung, Stuttgart, 1976:182-190.

[13] Omrani J, Agard P, Whitechurch H, Benoit M, Prouteau G, Jolivet L. Arc-magmatism and subduction history beneath the Zagros Mountains, Iran: A new report of adakites and geodynamic consequences. Lithos, 2008, 106: 380-98.

[14] Sabzehei M. Les mélanges ophiolitiques de la région d'Esfandagheh (Iran meridonal) étude pétrologique et structural, interpré- tation dans le cadre iranien, Thèse d'État, Université de Grenoble, 1974.

[15] Stocklin J. Possible ancient continental margins in Iran. In: Burk CA, Drake CL (Eds.), The geology of continental margins.Springer, Berlin, 1974: 873-887.

[16] Taraz H. Geology of the Surmaq-Deh Bid area, Abadeh region, Central Iran, Geological Survey of Iran, Report , 1974, 37: 37: 148.

[17] Maknouni Gilani S, Zare M and Raeisei E. Determining the hard rock groundwater pathway in Golgohar complex formation using hydrochemical data in AHP. Arabian Journal of Geosciences, 2018.
DOI: org/10.1007/s12517-018-3472-z, 11:172

[18] Maknouni Gilani S, Zare M and Raeisei E. Locating a New Drainage Well by Optimization of a Back Propagation. Mine Water and the Environment, 2019.
DOI: org/10.1007/s10230-019-00593-6

Author Guidelines

This document provides some guidelines to authors for submission in order to work towards a seamless submission process. While complete adherence to the following guidelines is not enforced, authors should note that following through with the guidelines will be helpful in expediting the copyediting and proofreading processes, and allow for improved readability during the review process.

Ⅰ. Format

- Program: Microsoft Word (preferred)
- Font: Times New Roman
- Size: 12
- Style: Normal
- Paragraph: Justified
- Required Documents

Ⅱ. Cover Letter

All articles should include a cover letter as a separate document.

The cover letter should include:

- Names and affiliation of author(s)

The corresponding author should be identified.

Eg. Department, University, Province/City/State, Postal Code, Country

- A brief description of the novelty and importance of the findings detailed in the paper

Declaration

v Conflict of Interest

Examples of conflicts of interest include (but are not limited to):

- Research grants
- Honoria
- Employment or consultation
- Project sponsors
- Author’s position on advisory boards or board of directors/management relationships
- Multiple affiliation
- Other financial relationships/support
- Informed Consent

This section confirms that written consent was obtained from all participants prior to the study.

- Ethical Approval

Eg. The paper received the ethical approval of XXX Ethics Committee.

- Trial Registration

Eg. Name of Trial Registry: Trial Registration Number

- Contributorship

The role(s) that each author undertook should be reflected in this section. This section affirms that each credited author has had a significant contribution to the article.

1. Main Manuscript
2. Reference List
3. Supplementary Data/Information

Supplementary figures, small tables, text etc.

As supplementary data/information is not copyedited/proofread, kindly ensure that the section is free from errors, and is presented clearly.

Ⅲ. Abstract

A general introduction to the research topic of the paper should be provided, along with a brief summary of its main results and implications. Kindly ensure the abstract is self-contained and remains readable to a wider audience. The abstract should also be kept to a maximum of 200 words.

Authors should also include 5-8 keywords after the abstract, separated by a semi-colon, avoiding the words already used in the title of the article.

Abstract and keywords should be reflected as font size 14.

Ⅳ. Title

The title should not exceed 50 words. Authors are encouraged to keep their titles succinct and relevant.

Titles should be reflected as font size 26, and in bold type.

Ⅳ. Section Headings

Section headings, sub-headings, and sub-subheadings should be differentiated by font size.

Section Headings: Font size 22, bold type

Sub-Headings: Font size 16, bold type

Sub-Subheadings: Font size 14, bold type

Main Manuscript Outline

Ⅴ. Introduction

The introduction should highlight the significance of the research conducted, in particular, in relation to current state of research in the field. A clear research objective should be conveyed within a single sentence.

Ⅵ. Methodology/Methods

In this section, the methods used to obtain the results in the paper should be clearly elucidated. This allows readers to be able to replicate the study in the future. Authors should ensure that any references made to other research or experiments should be clearly cited.

Ⅶ. Results

In this section, the results of experiments conducted should be detailed. The results should not be discussed at length in this section. Alternatively, Results and Discussion can also be combined to a single section.

Ⅷ. Discussion

In this section, the results of the experiments conducted can be discussed in detail. Authors should discuss the direct and indirect implications of their findings, and also discuss if the results obtain reflect the current state of research in the field. Applications for the research should be discussed in this section. Suggestions for future research can also be discussed in this section.

Ⅸ. Conclusion

This section offers closure for the paper. An effective conclusion will need to sum up the principal findings of the papers, and its implications for further research.

Ⅹ. References

References should be included as a separate page from the main manuscript. For parts of the manuscript that have referenced a particular source, a superscript (ie. [x]) should be included next to the referenced text.
[x] refers to the allocated number of the source under the Reference List (eg. [1], [2], [3])
In the References section, the corresponding source should be referenced as:
[x] Author(s). Article Title [Publication Type]. Journal Name, Vol. No., Issue No.: Page numbers. (DOI number)

Ⅺ. Glossary of Publication Type

J = Journal/Magazine

M = Monograph/Book

C = (Article) Collection

D = Dissertation/Thesis

P = Patent

S = Standards

N = Newspapers

R = Reports

Kindly note that the order of appearance of the referenced source should follow its order of appearance in the main manuscript.

Graphs, Figures, Tables, and Equations

Graphs, figures and tables should be labelled closely below it and aligned to the center. Each data presentation type should be labelled as Graph, Figure, or Table, and its sequence should be in running order, separate from each other.
Equations should be aligned to the left, and numbered with in running order with its number in parenthesis (aligned right).

Ⅻ. Others

Conflicts of interest, acknowledgements, and publication ethics should also be declared in the final version of the manuscript. Instructions have been provided as its counterpart under Cover Letter.

Hydro Science & Marine Engineering

Aims and Scope

Hydro Science & Marine Engineering publishes original research papers that offers professional review and publication to freely disseminate research findings in areas of Marine Biotechnology, Ocean Engineering, Irrigation and Drainage, Hydraulics and more. The Journal focuses on innovations of research methods at all stages and is committed to providing theoretical and practical experience for all those who are involved in these fields.

Hydro Science & Marine Engineering aims to discover innovative methods, theories and studies in its field by publishing original articles, case studies and comprehensive reviews.

The scope of the papers in this journal includes, but is not limited to:

- Marine Biotechnology
- Irrigation and Drainage
- Ocean Engineering
- Hydraulics
- Surface and Groundwater Hydrology
- Sediment Transport
- Climate Change
- Water Quality and Pollution control
- Coastal Protection
- Lake/Shore Environment
- Water Socio-Economics

Bilingual Publishing Co. (BPC)

Tel:+65 65881289

E-mail:contact@bilpublishing.com

Website:www.bilpublishing.com

About the Publisher

Bilingual Publishing Co. (BPC) is an international publisher of online, open access and scholarly peer-reviewed journals covering a wide range of academic disciplines including science, technology, medicine, engineering, education and social science. Reflecting the latest research from a broad sweep of subjects, our content is accessible world-wide——both in print and online.

BPC aims to provide an analytics as well as platform for information exchange and discussion that help organizations and professionals in advancing society for the betterment of mankind. BPC hopes to be indexed by well-known databases in order to expand its reach to the science community, and eventually grow to be a reputable publisher recognized by scholars and researchers around the world.

BPC adopts the Open Journal Systems, see on ojs.bilpublishing.com

Database Inclusion

Asia & Pacific Science Citation Index

Creative Commons

China National Knowledge Infrastructure

Google Scholar

Crossref

MyScienceWork

Bilingual Publishing Co. is a company registered in Singapore in 1984, whose office is at 12 Eu Tong Sen Street, #08-169, Singapore 059819, enjoying a high reputation in Southeast Asian countries, even around the world.

BILINGUAL PUBLISHING CO.
Pioneer of Global Academics Since 1984

Tel:+65 65881289
E-mail:contact@blipublishing.Com
Website:www.Blipublishing.Com

ISSN 2661-331X